Connecting two C_{60} stoppers to molecular wires: ultrafast intramolecular deactivation reactions†

Carmen Atienza,[a] Braulio Insuasty,[ab] Carlos Seoane,[a] Nazario Martín,*[a] Jeff Ramey,[c] G. M. Aminur Rahman[d] and Dirk M. Guldi*[c]

Received 5th August 2004, Accepted 12th November 2004
First published as an Advance Article on the web 26th November 2004
DOI: 10.1039/b412110d

A new series of soluble dumbbell-type architectures constituted by π-conjugated oligophenyleneethynylenes (OPEs) and two C_{60} stoppers have been prepared by using a convergent synthetic strategy. In particular, we base our approach on the systematic cross-coupling, palladium catalyzed Hagihara–Sonogashira reaction between aryl iodides and alkynyl derivatives. The cyclic voltammetry of the correspondingly synthesized system reveals amphoteric redox behavior and the lack of significant electronic communication between the oligo-arylalkynyl bridge and the two C_{60} moieties, which behave as two independent units. Excited state studies carried out by fluorescence and transition absorption spectroscopy show that, although a weak competitive electron transfer could operate in the deactivation process of the excited oligo-arylalkynyl bridges, their deactivation is mainly governed by energy transfer.

Introduction

"Molecular electronics" is currently a hot topic in chemistry, which requires the development of efficient synthetic methodologies to afford a wide variety of different chemical structures able to perform specific functions—wires, motors, diodes rectifiers antennas, *etc*.[1] The rational design of such functional molecules as well as the understanding of the physical processes occurring at the nanoscale molecular level are currently important challenges in science.[2] In particular, the study of π-conjugated oligomers has drawn interdisciplinary attention due to their broad applicability.[3] Thus, monodisperse π-conjugated oligomers of different nature [oligo-phenylenevinylenes (OPVs); oligo-thienylenevinylenes (OTVs); oligo-phenyleneethynylenes (OPEs); *etc*.] have been developed as simple model systems to mimic the more complex features of the respective π-conjuguted polymers as well as to test them as active components in optoelectronic devices.[4]

On the other hand, with the advent of fullerenes, and in particular of C_{60}, a new three-dimensional electron acceptor became available, which exhibits exciting characteristics. The delocalization of charges—electrons or holes—within the giant, spherical carbon framework (diameter > 7.5 Å) together with the rigid, confined structure of the fullerene sphere offers unique opportunities for stabilizing charged entities. Six equally spaced reduction waves in electrochemical experiments,[5] with the first reduction step resembling that of quinones—the electron acceptor unit in PRC proteins which is reduced to a semiquinone and finally to a hydroquinone—are a first manifestation for conditions that guarantee the optimal delocalization of charges. From this observation we infer the potential of fullerenes to posses quite small reorganization energies in electron transfer reactions, which renders an application of this carbon material as electron accepting moieties particularly appealing under aspects of energy conversion and energy storage.[6]

Recently, we and others have developed several different approaches towards the preparation of C_{60}/π-conjugated oligomer architectures as integrative building blocks for the efficient conversion of solar energy.[7] Interestingly, depending upon the electronic nature and length of the π-conjugated oligomer connected—either covalently or through supramolecular interactions—to C_{60}, different photophysical scenarios (*i.e.*, energy transfer *versus* electron transfer) evolved in the corresponding C_{60}–oligomer systems. However, in contrast to the large number of dyads (*i.e.*, C_{60}–oligomers), the number of triads (*i.e.*, C_{60}–oligomer–C_{60}) is considerably lower and only for a few of them (**T1**, **T2**) have their photophysical properties been studied and reported (Chart 1).[7,8]

We have recently shown that for C_{60}–OPV–C_{60} triads,[9a] although no significant differences were established for the general photoreactivity relative to the related C_{60}–OPV dyads,[9b] remarkable differences were found in their charge-separation features. In addition, we documented decisive evidence for molecular wire behavior through OPV systems.[10] These results prompted us to study other rigid and soluble C_{60}–oligomer–C_{60} dumbbell-type triads bearing rigid oligo-phenyleneethynylene (OPE) moieties with solubilizing alkoxy chains.

In this paper we wish to describe rational synthetic strategies en route towards functionalized oligomers, in which the oligomer length has been systematically increased from the monomer to the heptamer, as well as their electrochemical features, which were determined by cyclic voltammetry. The photophysical study of the novel compounds, as carried out by a series of fluorescence and transient absorption spectroscopic measurements, complements the present study to gain a better understanding of the excited state properties of the new triads.

† Electronic supplementary information (ESI) available: fluorescence spectra. See http://www.rsc.org/suppdata/jm/b4/b412110d/

*nazmar@quim.ucm.es (Nazario Martín)
dirk.guldi.@chemie.uni-erlangen.de (Dirk M. Guldi)

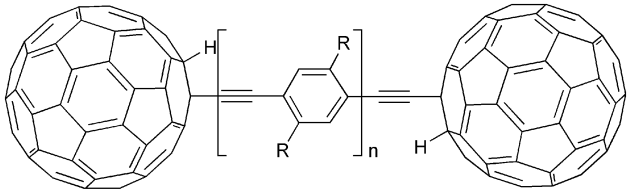

n=1,2,3,5 R=$OC_{10}H_{21}$ (**T1**)

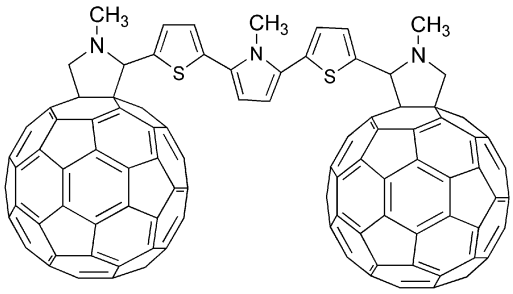

T2

Chart 1 C_{60}–oligomer–C_{60} triads (**T1** and **T2**).

Results and discussion

Synthesis

The synthesis of C_{60}–OPE–C_{60} is based on the preparation of π-conjugated oligo-phenyleneethynylenes (OPEs) that must meet two common features: i) the presence of solubilizing long chains, due to the well-known poor solubility of these rigid rod-like structures, and ii) the presence of functional groups at the terminal positions for further chemical reactions with, for example, C_{60}.

Ethynylation of C_{60} has been previously reported by Komatsu *et al.* as a general and versatile procedure which, however, seems to depend on the experimental conditions.[11] The ethynylation reaction has been successfully carried out by electrochemical procedures[12] and, more recently, by *in situ* generation of lithium acetylide in THF.[13] By following the last mentioned synthetic strategy, Tour and coworkers have recently reported a new series of C_{60}–OPE–C_{60} triads as well as other C_{60}/OPE hybrids bearing three fullerene units.[13]

In this work we report on the synthesis of novel C_{60}–OPE–C_{60} triads, in which the OPE moiety is covalently connected to two fullerenes through a pyrrolidine ring by using the efficient and widely used Prato procedure.[14] Therefore, the OPE precursors were functionalized with two terminal formyl groups which are, in turn, required for the formation of the respective azomethyne ylide intermediates. The synthetic strategy for the preparation of the different monodisperse OPEs (n = 1, 3, 5) is based on the design of suitable building blocks (**1–5**)—see Scheme 1—which were further used as starting materials in a convergent synthetic strategy.

The starting building blocks are shown in Scheme 1. Compounds **2–4** were prepared from diiodide **1**[15] and commercially available *p*-iodobenzaldehyde (**5**). To these compounds the respective ethynyl groups were introduced by using the Hagihara–Sonogashira reaction.[16] Compound **2**, for example, bearing an alkynyl unit was obtained from **1** and triisopropylsilylacetylene by cross-coupling reaction using

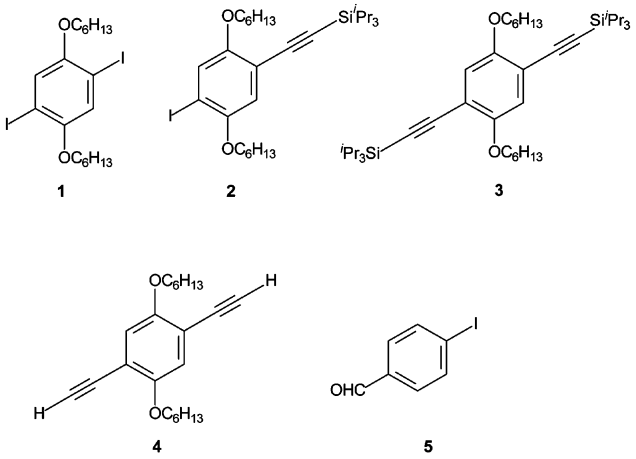

Scheme 1 Building blocks used in the preparation of OPEs.

palladium(II), copper(I) iodide and PPh_3 in piperidine at room temperature. Compound **3** was similarly obtained in a two-step reaction sequence. Further deprotection of **3**, by treatment with tetrabutylammonium fluoride in THF at room temperature, afforded **4** in 98% yield. With these starting building blocks (**1–5**) in hand, the preparation of the respective oligomers was carried out by means of the Hagihara–Sonogashira reaction, that is, using catalytic amounts of bis(triphenylphosphine)palladium dichloride, copper(I) iodide, and triphenylphosphine. The reactions were carried out in piperidine or, in some cases, piperidine–toluene to improve the solubility (see Experimental section) (Scheme 2).

Although some reactions were performed with the bromo- and iodo-arenes, the best results were obtained from the respective iodoarenes which reacted with the Pd(0)PPh_3 complexes generated *in situ* to give the alkynyl protected derivatives in good yields. In these reactions the piperidine acts as a solvent and, simultaneously, as a base to neutralize the hydrogen iodide formed in the reaction medium.[17] Thus, compound **6** (n = 3) bearing three repeating arylalkynyl units was prepared from **2** and **4** (n = 1) by using the above reaction conditions. Deprotection of **6** (n = 3), by fluoride treatment, led to the free ethynyl containing compound **7** (n = 3). Repetitive reactions of **2** with **7** (n = 3) under similar experimental conditions afforded compound **8** (n = 5) in 80% yield. Deprotection of **6** and **8** led to **7** (n = 3) and **9** (n = 5) in high yields (84% and 98%, respectively) (Scheme 2).

Formyl functionalized oligomers (OPEs) **10a–c** were then obtained by palladium(0) catalyzed Hagihara–Sonogashira reaction of *p*-iodobenzaldehyde (**5**) with the respective OPEs [**4** (n = 1); **7** (n = 3); **9** (n = 5)]. Some slight modifications of the experimental conditions were carried out (*i.e.*, use of diisopropylamine as solvent) in order to improve the yields—see Experimental section.

Finally, C_{60}–OPE(n)–C_{60} (n = 1, 3, 5) **11a–c** were prepared in moderate yields (*i.e.*, 20–43%) as stable brown solids by 1,3-dipolar cycloaddition reaction of the respective azomethyne ylides, generated *in situ* from dialdehydes **10a–c** and methyl or octyl *N*-substituted glycines, to C_{60} by heating at 130 °C in *o*-dichlorobenzene (ODCB).[14] *N*-Octylglycine is not commercially available and, therefore, it was synthesized by following

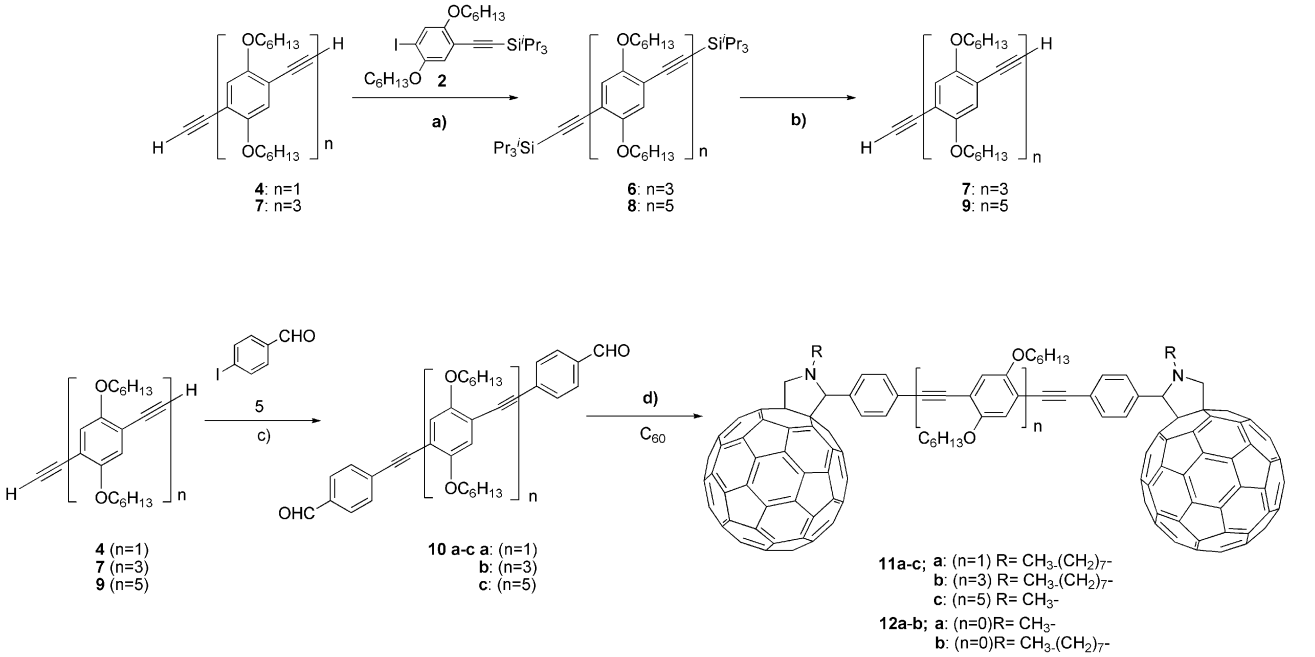

Scheme 2 *Reagents and conditions*: a) $Pd(PPh_3)_2Cl_2$, PPh_3, CuI, piperidine, rt, 24 h; b) Bu_4NF, THF, rt, 1 h; c) $Pd(PPh_3)_2Cl_2$, PPh_3, CuI, piperidine, rt, 24 h or $Pd(PPh_3)_4$, $^iPr_2NH$, THF, Δ, 16 h; d) *N*-octylglycine or sarcosine, ODCB, Δ, 3 h.

the procedure previously reported.[18] Compounds **12a–b** ($n = 0$) were prepared from commercially available 4,4′-diphenylethynyl dialdehyde (Scheme 2).[17] Although compounds **11a–c** and **12a–b** should be obtained as a stereoisomeric mixture due to the formation of two stereogenic centers in the two-fold cycloaddition reaction, high resolution ^1H NMR spectra (500 MHz) showed the presence of only one stereoisomer.

The final compounds (triads **11a–c**, **12**) as well as the functionalized intermediate oligomers (OPEs) (**6–10**) and starting building blocks (**1–5**) were fully characterized by spectroscopic and elemental analyses. MALDI and accurate mass analyses for triads **11a–c** were carried out to confirm the proposed structures.

Electrochemistry

The redox properties of the novel triads as well as the oligomeric precursors OPE($n = 3$) (**6**) and OPE($n = 5$) (**8**), were determined by cyclic voltammetry at room temperature in ODCB–CH_3CN (4 : 1) with a platinum wire as working electrode. In all cases tetrabutylammonium perchlorate was used as supporting electrolyte and the scan rate was 100 mV s^{-1}. The experimental data are collected in Table 1 together with those of C_{60} as reference.

All the new triads showed amphoteric redox behavior which is rationalized by the presence of both donor (OPEs) and acceptor (C_{60}) moieties. It is interesting to note that despite the presence of two C_{60} units connected through a π-conjugated bridge, no electronic communication between them was electrochemically observed in the ground state. In line with this assumption, only three quasireversible reduction waves were observed in the cyclic voltammogram, corresponding to the first three reduction steps of C_{60}. This finding is in agreement with other related C_{60}–oligomer–C_{60} triads, which show a similar trend despite the different nature of the π-conjugated spacer.[9,13,19] As expected, the reduction waves are cathodically shifted in comparison with the parent C_{60} molecule. This is due to the saturation of the double bond, which raises the LUMO energy.[5,20] An additional weak reduction wave was observed for compounds **11a–c** at around −1.25 V, which corresponds to the reduction of the OPE unit. In contrast to that recently observed for the reduction waves of the C_{60} unit in triads **T1**, the increasing chain length of the OPEs in **11a–c**, **12a–b** does not have an appreciable influence on the reduction potential values of the fullerene moieties. This fact could be accounted for by the two sp^3 carbon atoms existing between the C_{60} and the π-conjugated oligomer in compounds **11a–c**, **12**, whereas only one sp^3 carbon atom exists in triads **T1**.[13]

On the oxidation side, triads **11a–c** showed the presence of an oxidation wave at around 1.40 V, which relates to the oxidation process of the OPE moiety. This oxidation wave is slightly cathodically shifted with increasing the length of the oligomer. However, this wave was not observed in triad **12b**

Table 1 Redox potential values (±0.01 V) for compounds (V *vs.* Ag/Ag^+)[a]

Comp.	E_{ox}	E^1_{red}	E^2_{red}	E^3_{red}	E^4_{red}	E^5_{red}	E^6_{red}
C_{60}	—	−0.53	−0.94	—	−1.42	—	−1.91
6	1.35; 1.57	—	—	—	—	−1.72	−1.93
8	1.27; 1.54	—	—	—	—	−1.73	−1.92
11a	1.46	−0.63	−1.02	−1.30	−1.57	—	—
11b	1.43	−0.61	−1.01	[b]	−1.53	—	—
11c	1.37	−0.59	−1.00	−1.24	−1.55	—	−1.80
12b	—	−0.61	−0.99	—	−1.54	—	—

[a] Experimental conditions: ODCB–CH_3CN 4 : 1 as solvent, Pt as working electrode, Bu_4NClO_4 (0.1 M) as supporting electrolyte; 100 mV s^{-1}. [b] No clear signal was observed.

due to the weak electron donor ability of the diphenylacetylene moiety. This oxidation wave was also observed for the parent oligomers **6** and **8**, which showed a first oxidation potential at 1.35 and 1.27 V, respectively. For these oligomers, a second oxidation wave was observed at around 1.5 V which, however, is not present in triads **11a–c** (Table 1). In addition, oligomers **6** and **8** showed a weak reduction wave at around −1.90 V which was, however, only observed in triad **11c**. In summary, the cyclic voltammetry data reveal the lack of significant electronic interaction between the electroactive units OPE and C_{60} in the ground state.

Photophysics

First we tested the excited state features of the reference compounds that make up the family of novel C_{60}–wire–C_{60} systems (*i.e.*, C_{60} and phenylene-acetylene blocks of variable length). For details on the C_{60} features we refer the reader to the extensive literature.[21] Within the context of the current studies, only the weak fluorescing features that are maximized at 710 nm and the strong triplet–triplet transitions at 360 and 700 nm should be mentioned explicitly.

Much less information is available on the phenylene-acetylene building blocks. The major features include strong visible light fluorescence with quantum yields close to unity (*i.e.*, **10a**: 0.75; **10b**: 0.78; **10c**: 0.77). The fluorescence maxima, similarly to the absorption maxima, depend on the length of the π-conjugated oligo-phenyleneethynylenes and reach from 400 nm to 490 nm (*i.e.*, electronic supplementary information†–Fig. S1), in case of the monomer and heptamer, respectively. Interestingly, the fluorescence lifetimes are also influenced by the length of the π-conjugated oligo-phenyleneethynylenes with values of 2.3 ± 0.1 ns (**10a**), 0.71 ± 0.02 ns (**10b**) and 0.6 ± 0.02 ns (**10c**). The product of this relatively slow singlet excited state decay is the phenylene-acetylene triplet. Spectroscopic characteristics of the triplet–triplet spectra are maximized around 650 nm. These shift typically to the red with increasing phenylene-acetylene length.[22]

When comparing the absorption spectra of the reference systems, we note that the phenylene-acetylene building blocks dominate most of the visible spectrum (*i.e.*, 300–600 nm), where the C_{60} absorption is marginal. Only in the UV range is the C_{60} absorption cross section competitive. Relative to the sum of the references, some degree of perturbation is found for the C_{60}–wire–C_{60} spectra. Implicit here are appreciable electronic couplings between the different building blocks. This, in turn, is expected to influence the deactivation rates. In summary, visible light excitation of **11a–c** will reach exclusively the phenylene-acetylenes.

Insight into intramolecular deactivation processes came from emission assays, namely, steady-state and time-resolved fluorescence experiments. In particular, we compared the strongly emissive features of the phenylene-acetylene units in the 500–700 nm range upon photoexciting (*i.e.*, in the visible at 390 nm) the references and **11a–c** – see Fig. 1a and b. Dramatic differences in the fluorescence quantum yields between the references and **11a–c**, that are as large as 1500, attest to an almost instantaneous deactivation of the quantitatively excited phenylene-acetylene building blocks. When inspecting the

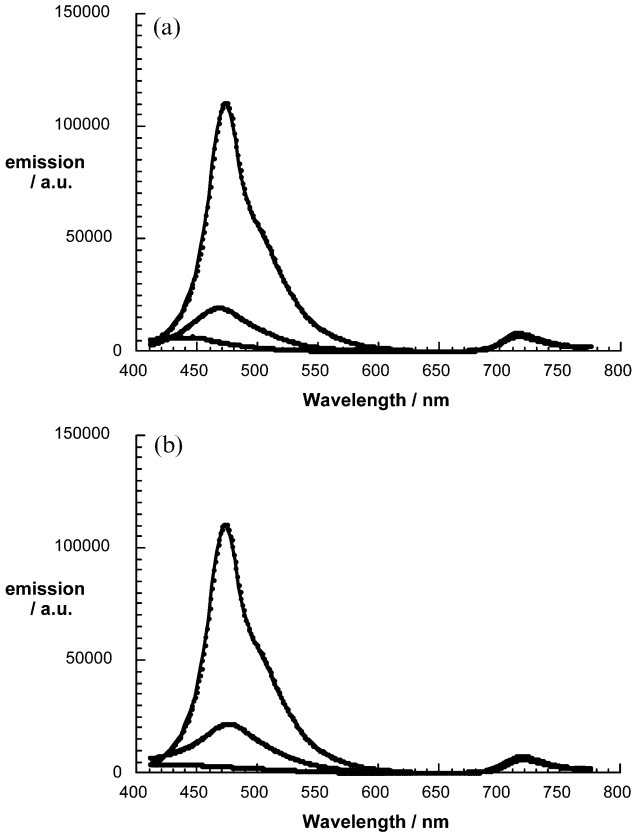

Fig. 1 a: Fluorescence spectra of **11c**, **11b**, and **11a**—in order of decreasing fluorescence intensity— in toluene with matching absorption at the 390 nm excitation wavelength (*i.e.*, $OD_{390\ nm}$ = 0.2). b: Fluorescence spectra of **11c**, **11b**, and **11a**—in order of decreasing fluorescence intensity—in benzonitrile with matching absorption at the 390 nm excitation wavelength (*i.e.*, $OD_{390\ nm}$ = 0.2).

700–800 nm range of the emission spectra a new transition emerges. In toluene, the latter is a quantitative (*i.e.*, quantum yield: 6×10^{-4}) and qualitative (*i.e.*, fluorescence maximum: 710 nm) match of the C_{60} reference fluorescence. A likely rationale for i) the absence of phenylene-acetylene fluorescence and ii) the presence of C_{60} fluorescence implies an exothermic transduction of the singlet excited state to the low lying C_{60} singlet excited state. Conclusive evidence for the fluorescence trapping came from excitation spectra, that is, probing the C_{60} emission at 710 nm as a function of excitation wavelength. The excitation spectra resemble the ground state absorption of the phenylene-acetylene building blocks, with broad maxima in the visible (*i.e.*, 350–450 nm). Taking this evidence into account we reach the conclusion that the origin of excited state energy is unquestionably that of the conjugated π-systems. Furthermore, it allows the underlying mechanism to be attributed: an efficient intramolecular transfer of singlet excited state energy from the photoexcited phenylene-acetylenes to the covalently linked fullerene governs the photophysics in **11a–c**.

In parallel fluorescence lifetime experiments, we made two major observations. Firstly, in the visible region (*i.e.*, 500–700 nm), where typically the long-lived phenylene-acetylene fluorescence dominates, no appreciable signal was seen that

falls within our 100 ps time window. In other words, the fluorescence deactivation in **11a–c** is faster than 100 ps ($k > 10^{10}$ s^{-1}), a consequence of the strong electronic coupling. Secondly, in the near-infrared region (*i.e.*, 700–800 nm) the fluorescence that originates from the C_{60} termini reveals lifetimes on the order of 1.5 $\pm$ 2 ns. These observations complement the steady-state experiments nicely.

We also probed **11a–c** in more polar media, such as THF and benzonitrile. Minor differences, relative to toluene, include slightly lower fluorescence quantum yields and slightly faster fluorescence deactivation of the C_{60} contributions. In line with previous reports on various C_{60}–oligomer and C_{60}–oligomer–C_{60} systems (*i.e.*, oligomer: phenylene-vinylene, *etc.*),[23] a competitive electron transfer deactivation is responsible for this trend. As can be deduced from the absolute differences in quantum yields, the electron transfer involvement is, however, small (*i.e.*, less than 5%). The phenylene-acetylene part, on the other hand, remains virtually unchanged. It is important to consider that solvent changes from toluene (ε = 2.38) to benzonitrile (ε = 24.8) lead to marked increases in free reaction enthalpy ($-\Delta G_{CS}^{\circ}$) for intramolecular electron transfer events, but to no or very little impact on that for energy transfer. Better solvation of radical ion pairs assists in a polar solvent in lowering the energy of the electron transfer product, namely, the charge-separated radical ion pair. The excited states of C_{60} and phenylene-acetylene experience effects that are not worth mentioning. Thus, the noted tendency serves as an independent, indirect verification of excited state deactivation that is governed in large part by energy transfer, that is, at least 95%.

A thermodynamic consideration sheds light onto our experimental observation. As a test to validate the above conclusion, the driving forces ($-\Delta G_{CS}^{\circ}$), associated with an intramolecular charge separation in **11a–c**, were calculated in accordance with the following approximation:[24]

$$-\Delta G_{CS}^{\circ} = -\{e[E_{1/2}(\text{phenylene-acetylene}^{\bullet+}/\text{phenylene-acetylene}) - E_{1/2}(C_{60}/C_{60}^{\bullet-})] - \Delta E^{*}_{0\text{-}0}\} \quad (1)$$

$E_{1/2}$(phenylene-acetylene$^{\bullet+}$/phenylene-acetylene) and $E_{1/2}$-($C_{60}/C_{60}^{\bullet-}$) correspond to the standard potentials for the oxidation and reduction of phenylene-acetylene and C_{60}, respectively (see Table 1), while $\Delta E^{*}_{0\text{-}0}$ represents the energy of the photoexcited phenylene-acetylene singlet excited state and e is the elementary charge. Considering, however, the energy of the fullerene singlet excited state of 1.76 eV, relative to those of the charge-separated state (in ODCB–CH_3CN 4 : 1, >2.0 eV), it is clear that the largest energy gap opens between the two singlet excited states (*i.e.*, phenylene-acetylene and fullerene). Consequently, the energy transfer route is the thermodynamically favored pathway. From this cause we can assume that, once populated, after the completion of the singlet–singlet energy transfer, the fullerene singlet excited state can only decay to the triplet excited state and finally to the singlet ground state—see the schematic sketch in Fig. 2. Comparing the overall photoreactivity of **11a–c** to previous reports on C_{60}–oligomer and C_{60}–oligomer–C_{60} systems,[7–9,11,12] intramolecular transduction of singlet excited state energy to the energetic sink (*i.e*, C_{60}) is a common reaction pathway.

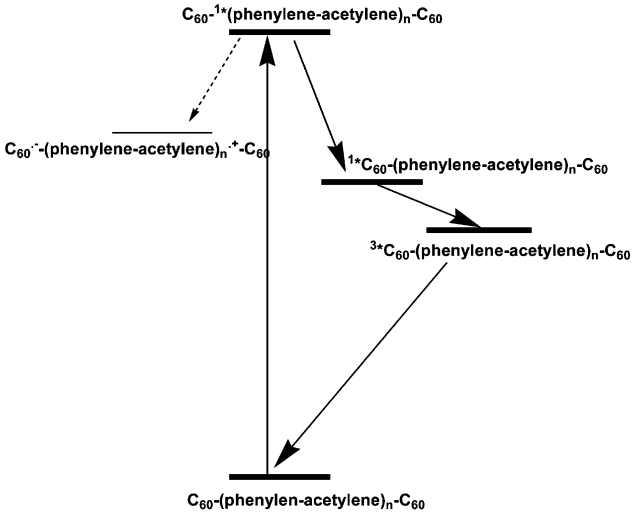

Fig. 2 Schematic illustration of the reaction pathways in photo-excited **11a–11c**.

In the next step we employed transient absorption spectroscopy to test the product of the singlet–singlet transfer in **11a–c**. With the conclusion of nanosecond laser excitation at 308, 337 or 355 nm, spectroscopic and kinetic analyses suggest the formation of just one photo-product. Spectroscopically, transient maxima at 360 and 700 nm are unmistakable attributes of a C_{60} triplet–triplet spectrum—see Fig. 3.[23] Kinetically, we see transient decays that are best fitted by a complex mixture of uni- and bimolecular dynamics with an average lifetime of ~20 microseconds. Again, this fits the picture seen for the C_{60} reference under identical experimental conditions. For example, lowering the concentration of **11a–c** and/or decreasing the laser flux leads to longer C_{60} triplet lifetimes, while raising the concentration of **11a–c** and/or increasing the laser power resulted in shorter lifetimes, due to variable contributions from intermolecular triplet–triplet annihilations.

Interestingly—regardless of the solvent—in the 1000 nm region, where the radical anion fingerprint of C_{60} (*i.e.*, $C_{60}^{\bullet-}$) absorbs, no evidence for a significant contribution of electron

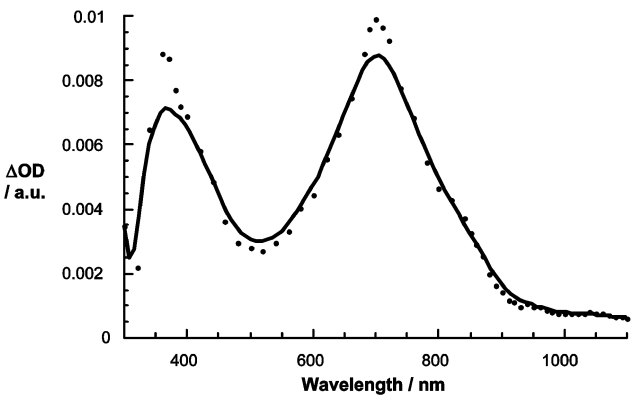

Fig. 3 Transient absorption spectrum (*i.e.*, visible-near-infrared part) recorded 100 ns upon flash photolysis of **11c** (2.0×10^{-5} M) at 355 nm in deoxygenated benzonitrile, showing the fullerene triplet–triplet features (λ_{max} = 360 and 700 nm).

transfer was gathered. Also C_{60} triplet quantum yields of unity are nearly the same in the C_{60} reference and **11a–c**.

Conclusions

In summary, we have carried out the synthesis of novel C_{60}-based dumbbell-type triads in which highly soluble π-conjugated oligophenyleneethynylenes (OPEs) are covalently connected to two C_{60} units. The length of the OPEs has been systematically increased by using a cross-coupling palladium catalysed Hagihara–Sonogashira reaction of aryl iodides and alkynyl derivatives. Finally, the two formyl containing OPEs at terminal positions were reacted with C_{60} by following Prato's methodology to afford the novel series of triads. In agreement with previous studies, the cyclic voltammetry of **11a–c** and **12b** showed that no significant electronic interaction takes place between the two C_{60} units in the ground state, which behave as two independent systems. Photophysical studies carried out by fluorescence and transition absorption spectroscopy revealed that despite the good electron donor features of the oligomer, the energy of the C_{60} singlet excited state drops below the energy of the resulting charge-separated radical ion pair features that are similar to comparable C_{60}–oligomer and C_{60}–oligomer–C_{60} systems.[7–9,11,12] Thus, we see an outcome that is dominated by an intramolecular energy transfer reaction, which thermodynamically (*i.e.*, larger energy gap) and mechanistically (*i.e.*, efficient dipole–dipole interactions) prevails.

Experimental

Picosecond laser flash photolysis experiments were carried out with 355 nm laser pulses from a mode-locked, Q-switched Quantel YG-501 DP Nd : YAG laser system (pulse width 18 ps, 2–3 mJ pulse^{-1}). The white continuum picosecond probe pulse was generated by passing the fundamental output through a D_2O–H_2O solution. The excitation and the probe was fed to a spectrograph (HR-320, ISDA Instruments, Inc.) with fiber-optic cables and was analyzed with a dual diode array detector (Princeton Instruments, Inc.) interfaced with an IBM-AT computer.

Nanosecond laser flash photolysis experiments were performed with laser pulses from a Molectron UV-400 nitrogen laser system (337.1 nm, 8 ns pulse width, 1 mJ pulse^{-1}). The photomultiplier output was digitized with a Tektronix 7912 AD programmable digitizer. A typical experiment consisted of 5–10 replicate pulses per measurement. The averaged signal was processed with an LSI-11 microprocessor interfaced with a VAX-370 computer.

Time-resolved emission fluorescence lifetimes were measured with a Laser Strope Fluorescence Lifetime Spectrometer (Photon Technology International) with 337 nm laser pulses from a nitrogen laser fiber-coupled to a lens-based T-formal sample compartment equipped with a stroboscopic detector. Details of the Laser Strobe systems are described on the manufacturer's web site, http://www.pti-nj.com.

Steady-state emission and excitation spectra were recorded with a SLM 8100 Spectrofluorometer. Fluorescence spectra were measured in methylcyclohexane solutions containing fullerene forming clear, non-cracking glasses in liquid nitrogen. In case of any other solvents, the experiments were performed at room temperature. A 570 nm long-pass filter in the emission path was used in order to eliminate the interference from the solvent and stray light for recording the fullerene fluorescence. No corrections were performed for the fluorescence, but long integration times (20 s) and low increments (0.1 nm) were applied. The slits were 2 and 8 nm and each spectrum was an average of at least 5 individual scans.

Synthesis and characterization

IR spectra were recorded in KBr pellets. ^{1}H and ^{13}C NMR spectra were recorded at 500, 300, 200 and 125, 75, 50 MHz respectively; chemical shifts are given as δ values (int. standard: TMS). Cyclic voltammograms were recorded on a potentiostat/galvanostat equipped with a software electrochemical analysis Model 250 by using platinum as working electrode, SCE as reference electrode, $Bu_4N^+ClO_4^-$ as supporting electrolyte, ODCB–CH_3CN as solvent, and at a scan rate of 100 mV s^{-1}.

Triad 12a

C_{60} (360 mg, 0.5 mmol) was dissolved in chlorobenzene (ultrasound 30 min), 4,4′-diphenylethynyl dialdehyde (58.5 mg, 0.25 mmol) and sarcosine (133.6 mg, 1.5 mmol) was added. The mixture was heated under reflux for 10 h. After the evaporation the solvent, the residue was purified by column chromatography on silica gel (CS_2–toluene 5 : 2). Yield 58% of black solid. Compound insoluble.

Triad 12b

C_{60} (360 mg, 0.5 mmol) was dissolved in chlorobenzene (ultrasound 30 min), 4,4′-diphenylethynyl dialdehyde (58.5 mg, 0.25 mmol) and *N*-octylglycine (280 mg, 1.5 mmol) was added. The mixture was heated under reflux for 10 h. After the evaporation of the solvent, the residue was purified by column chromatography on silica gel (CS_2–toluene 5 : 2). Yield 58% of black solid. ^{1}H NMR (500 MHz, $CDCl_3$) δ: 7.92 (brs, 4H), 7.67–7.65 (dd, J = 8.22 Hz, 4H), 5.27 (d, J = 9.18 Hz, 2H), 5.22 (s, 2H), 4.30 (dd, J = 9.2 Hz, 2H), 3.42–3.40 (m, 4H), 2.75 (m, 4H), 2.18 (m, 2H), 2.07 (m, 2H), 1.86 (m, 4H), 1.73 (m, 4H), 1.63 (m, 4H), 1.55 (m, 4H), 1.22 (m, 6H). ^{13}C NMR (125 MHz, $CDCl_3$) δ: 156.72, 154.49, 153.70, 153.49, 147.90, 147.88, 147.20, 146.97, 146.95, 146.87, 146.83, 146.79, 146.76, 146.71, 146.60, 146.56, 146.34, 146.24, 146.21, 146.07, 146.06, 145.96, 145.93, 145.89, 145.86, 145.84, 145.77, 145.32, 145.28, 145.01, 144.99, 143.79, 143.74, 143.66, 143.34, 143.25, 143.22, 143.21, 142.90, 142.87, 142.77, 142.72, 142.67, 142.66, 142.63, 142.50, 142.49, 142.32, 142.20, 140.90, 140.89, 140.65, 140.22, 138.17, 137.49, 137.17, 136.51, 136.34, 136.31, 132.65, 129.95, 124.29, 91.32, 83.04, 77.14, 69.38, 67.56, 54.12, 33.12, 30.89, 30.59, 29.57, 28.70, 24.13, 15.45. FTIR (KBr) ν 2918, 1848, 526 cm^{-1}. λ_{max} (CH_2Cl_2): 431, 321.02, 257.01 nm.

Compound 10a

Compound **4** (600 mg, 1.84 mmol) and compound **5** (852.8 mg, 3.68 mmol) were dissolved in dry piperidine (20 mL), and the

system was flushed with argon. Bis(triphenylphospine)-palladium dichloride (64.48 mg, 0.092 mmol), copper(I) iodine (19.69 mg, 0.1 mmol) and triphenylphosphine (29.96 mg, 0.1 mmol) were added. The mixture was stirred for 24 h at room temperature. Chloroform was added to the residue and washed with saturated NH_4Cl, neutralized with saturated HCl 10% and washed with NaCl. The organic phase was dried with $MgSO_4$ and the solvent was removed. The crude product was purified by column chromatography on silica gel, hexane–AcOEt (9 : 1).Yield 61% of yellow solid. Mp 125–126 °C. ^{1}H NMR (200 MHz, $CDCl_3$) δ: 10.02 (s, 2H), 7.89–7.85 (dd, J = 8.55 Hz, 2H), 7.69–7.65 (dd, J = 8.05 Hz, 2H), 7.04 (s, 2H), 4.08–4.02 (t, J = 6.35 Hz, 4H), 1.93–1.80 (m, 4H), 1.57–1.25 (m, 12H), 0.93–0.86 (m, 6H). ^{13}C NMR (50 MHz, $CDCl_3$) δ: 191.32, 153.89, 135.45, 132.03, 129.67, 129.56, 116.90, 113.96, 94.24, 90.01, 69.65, 31.56, 29.26, 25.73, 22.61, 13.99. EM m/z 543 (100), 463 (9), 450 (15), 379 (19), 366 (100). FTIR (KBr) ν 1218, 1282, 1697, 2320, 2570 cm^{-1}. λ_{max} 395.99; 327.92 nm. Anal. Calcd for $C_{36}H_{38}O_4$: C 80.87, H 7.16, O 11.97. Found: C 80.95, H 7.16%.

Triad 11a

To a solution of C_{60} (360 mg, 0.5 mmol) in chlorobenzene (100 mL), compound **10a** (58.5 mg, 0.25 mmol) and *N*-octylglycine (280 mg, 1.5 mmol) was added. The mixture was heated under reflux for 10 h. After evaporation of the solvent, the residue was purified by column chromatography on silica gel (CS_2–toluene 5 : 2). Yield 43% of black solid. ^{1}H NMR (500 MHz, $CDCl_3$) δ: 7.71 (brs, 4H), 7.50–7.49 (dd, J = 8.37 Hz, 4H), 6.89 (s, 2H), 5.04–5.00 (m, 4H), 4.07–4.02 (m, 2H), 3.92–3.81 (m, 4H), 3.15–3.13 (m, 4H), 2.50–1.91 (m, 4H), 1.91–1.81 (m, 4H), 1.80–1.70 (m, 8H), 1.58–1.53 (m, 4H), 1.47–1.17 (m, 20H), 0.85–0.71 (m, 12H). ^{13}C NMR (125 MHz, $CDCl_3$) δ: 156.41, 154.12, 153.57, 153.28, 147.29, 146.65, 146.41, 146.29, 146.20, 146.14, 146.01, 145.92, 145.73, 145.51, 145.31, 145.24, 145.15, 144.70, 144.61, 144.37, 143.14, 142.97, 142.66, 142.55, 142.29, 142.23, 142.12, 142.01, 141.86, 141.65, 141.51, 140.16, 140.12, 139.85, 139.52, 137.73, 136.90, 136.54, 135.81, 135.64, 131.81, 129.41, 123.43, 116.84, 113.86, 94.70, 86.67, 82.31, 69.57, 68.88, 66.80, 53.23, 31.91, 31.54, 29.54, 29.32, 29.22, 28.28, 27.54, 25.68, 22.71, 22.61, 14.16, 14.06. FTIR (KBr) ν 526, 1375, 279, 2848 cm^{-1}. λ_{max} (CH_2Cl_2): 431, 371.97, 266.92 nm. EM (MALDI-TOF) m/z 2226.60.

Tris(2,5-dihexyloxy-1,4-triisopropylsilylethynylbenzyl)benzene. 6

Compounds **4** (326 mg, 1 mmol) and **2** (1.168 mg, 2 mmol) were dissolved in dry piperidine (20 mL) and the system was flushed with argon. Bis(triphenylphosphine) dichloride (35.09 mg, 0.005 mmol), copper(I) iodide (19.04 mg, 0.1 mmol) and triphenylphosphine (26.23 mg, 0.1 mmol) were added. The mixture was stirred for 48 h at room temperature. Chloroform was added and washed with NH_4Cl, neutralized with saturated HCl 10% and washed with NaCl. The organic phase was dried with $MgSO_4$ and the solvent was removed. The crude product was purified by column chromatography on silica gel, using toluene as the eluent. Yield 78% of yellow solid. Mp 100–101 °C. ^{1}H NMR (200 MHz, $CDCl_3$) δ: 6.99–6.97 (brs, 2H), 6.96 (brs, 2H), 6.93 (brs, 2H), 4.13–3.91 (m, 12H), 1.86–1.54 (m, 12H), 1.34–0.88 (m, 60H), 0.0053 (s, 36H). ^{13}C NMR (50 MHz, $CDCl_3$) δ: 154.35, 153.53, 153.34, 153.28, 118.02, 117.30, 116.64, 114.45, 114.34, 114.23, 114.05, 69.89, 69.70, 69.30, 31.66, 31.60, 29.43, 29.31, 25.83, 25.64, 22.60, 18.69, 14.02, 13.98, 11.39, 0.98. FTIR (KBr) ν 636, 657, 677, 769 , 812, 1029, 1211, 1274, 1340, 1386, 1419, 1458, 1473, 2148, 2864, 2941 cm^{-1}. EM m/z 1238, 1132, 1131, 1050, 685. λ_{max} (CH_2Cl_2): 417; 315 nm. Anal. Calcd for $C_{80}H_{126}O_6Si_2$: C 77.49, H 10.24, O 7.74. Found: C 78.19, H 9.89%.

Tris(2,5-dihexyloxy-1,4-(ethynylbenzyl)benzene 7

Compound **6** (1.238 mg, 1 mmol) was dissolved in THF (30 mL) and tetrabutylammonium fluoride (574.2 mg, 2.2 mmol) was added to the solution. The solution was stirred at room temperature for 10 h. The mixture was extracted with chloroform and washed with water. The organic phase was dried with $MgSO_4$. The solvent was removed and the product was crystallized with hexane. Yield 84% of yellow solid. ^{1}H NMR (200 MHz, $CDCl_3$) δ: 7–6.97 (brs, 6H), 4.04–3.96 (m, 12H), 3.34 (s, 2H), 1.86–1.80 (m, 12H), 1.55–1.25 (m, 36H), 0.90–0.87 (m, 18H). ^{13}C NMR (50 MHz, $CDCl_3$) δ: 154.17, 153.55, 153.34, 118.02, 117.33, 117.12, 115.01, 114.33, 112.63, 91.54, 80.04, 69.71, 69.65, 31.58, 31.51, 29.29, 29.24, 29.14, 25.63, 25.59, 22.60, 22.56, 13.98. FTIR (KBr) ν 601, 640, 860, 1062, 1220, 1346, 1384, 1464, 1496, 2854, 2925, 2950 cm^{-1}.

Compound 10b

Compound **7** (920 mg, 1 mmol) and **5** (464 mg, 2 mmol) were dissolved in dry piperidine (20 mL) and toluene (6 mL), the system was flushed with argon. Bis(triphenylphosphine)-palladium dichloride (35.09 mg, 0.05 mmol), copper(I) iodine (18.66 mg, 0.098 mmol) and triphenylphosphine (25.70 mg, 0.098 mmol) were added. The mixture was stirred for 48 h at room temperature. Chloroform was added to the residue and washed with saturated NH_4Cl, HCl (10%) and NaCl. The organic phase was dried with $MgSO_4$ and the solvent was removed. The crude product was purified by column chromatography on silica gel, hexane–AcOEt (9 : 1). Yield 84% of yellow-orange solid. Mp 119–120 °C. ^{1}H NMR (200 MHz, $CDCl_3$) δ: 10–02 (s, 2H), 7.89–7.84 (dd, J = 8.3 Hz, 4H), 7.68–7.64 (dd, J = 8.05 Hz, 4H), 3.96–3.91 (m, 12H), 1.89–1.82 (m, 12H), 1.56–1.51 (m, 12H), 1.36–1.25 (m, 24H), 0.91–0.88 (m, 18H). ^{13}C NMR (50 MHz, $CDCl_3$) δ: 191.34, 155.00, 153.94, 153.58, 153.50, 153.40, 135.35, 131.98, 129.82, 129.55, 117.85, 117.16, 117.03, 115.29, 114.35, 113.04, 91.98, 91.42, 90.27, 69.80, 69.72, 69.56, 31.58, 29.30, 25.75, 25.65, 22.61, 22.58, 14.00. FTIR (KBr) ν 731, 777, 1024 (m), 1217 (s), 1274 (m), 1386 (m), 1493 (m), 1596 (m), 1654 (m), 1701 (s), 2854 (s), 2925 (s) cm^{-1}. EM m/z 1158, 1135, 925, 737, 612, 296. λ_{max} (CH_2Cl_2): 434.99, 329.02, 274.97 nm. Anal. Calcd for $C_{76}H_{94}O_8$: C 80.38, H 8.34. Found: C 80.35, H 8.83%.

Triad 11b

C_{60} (360 mg, 0.5 mmol) was dissolved in chlorobenzene (100 mL), compound **10b** (58.5 mg, 0.25 mmol) and *N*-octylglycine (280 mg, 1.5 mmol) was added. The mixture

was heated under reflux for 10 h. After the evaporation the solvent, the residue was purified by column chromatography on silica gel (CS_2–toluene 5 : 2). Yield 35% of black solid. ^{1}H NMR (500 MHz, $CDCl_3$) δ: 7.73 (brs, 4H), 7.52–7.50 (d, J = 8.37 Hz, 4H), 6.91–6.89 (s, 6H), 5.05–5.01 (m, 4H), 4.07–4.02 (m, 2H), 3.94–3.89 (m, 12H), 3.16–3.15 (m, 4H), 2.51 (m, 4H), 1.91–1.81 (m,4H), 1.79–1.72 (m,16H), 1.59–1.17 (m, 48H), 0.85–0.71 (m,24H). ^{13}C NMR (125 MHz, $CDCl_3$) δ: 156.31, 154.95, 154.75, 154.03, 153.60, 153.48, 153.30, 147.30, 146.63, 146.39, 146.30, 146.25, 146.20, 146.14, 146.00, 145.93, 145.74, 145.51, 145.31, 145.25, 145.16, 144.70, 144.62, 144.37, 143.14, 142.97, 142.67, 142.56, 142.28, 142.22, 142.13, 142.01, 141.87, 141.65, 141.51, 140.12, 139.86, 139.53, 137.75, 136.95, 136.58, 135.79, 135.63, 131.82, 129.44, 123.50, 117.79, 117.63, 117.22, 117.03, 115.35, 114.40, 114.26, 113.92, 113.73, 112.54, 94.62, 92.11, 91.60, 91.48, 91.39, 86.77, 82.32, 79.92, 79.59, 79.33, 69.66, 69.56, 68.86, 66.76, 53.26, 31.58, 30.92, 29.60, 29.32, 29.25, 29.10, 28.22, 27.53, 25.69, 25.63, 22.71, 22.61, 14.15, 14.01. FTIR (KBr) ν 549, 1186, 2395 cm^{-1}. λ_{max} (CH_2Cl_2): 420.06, 321.96, 254.96 nm. EM (MALDI-TOF) m/z 2825.01.

Compound 8

Compound **7** (820 mg, 1 mmol) and **2** (1.096 mg, 2 mmol) were dissolved in dry piperidine (20 mL) and toluene (20 mL). The system was flushed with argon. Bis(triphenylphosphine)-palladium dichloride (35.09 mg, 0.05 mmol), copper(I) iodide (19.04 mg, 0.1 mmol) and triphenylphosphine (26.23 mg, 0.1 mmol) were added. The mixture was stirred for 48 h at room temperature. The residue was washed with saturated NH_4Cl, HCl (10%), NaCl and extracted with chloroform. The organic phase was dried with $MgSO_4$. The crude was purified by column chromatography on silica gel, using toluene as eluent. Yield 80% of yellow solid, mp 118–119 °C. ^{1}H NMR (300 MHz, $CDCl_3$) δ: 7.02–6.95 (brs, 10H), 4.06–3.93 (m, 20H), 1.88–1.75 (m, 20H), 1.53–1.36 (m, 20H), 1.35–1.14 (m, 40H), 0.92–0.88 (m, 30H). ^{13}C NMR (75 MHz, $CDCl_3$) δ: 155.45, 155.38, 155.17, 155.10, 154.74, 153.95, 153.90, 153.72, 153.65, 152.91, 151.96, 131.31, 129.23, 123.63, 119.73, 118.27, 118.19, 118.02, 117.60, 117.44, 117.10, 116.90, 116.62, 115.93, 115.82, 114.88, 114.76, 114.69, 114.66, 114.45, 114.41, 114.38, 114.09, 114.03, 113.83, 112.92, 103.61, 103.43, 103.00, 96.91, 96.52, 96.18, 94.78, 92.66, 92.12, 92.03, 92.00, 91.76, 88.03, 80.02, 79.76, 77.64, 70.58, 70.21, 70.12, 69.92, 69.79, 69.62, 69.08, 32.11, 32.04, 31.95, 30.12, 29.92, 29.85, 29.78, 29.71, 29.62, 29.57, 29.53, 29.44, 26.28, 26.09, 26.04, 23.05, 23.02, 19.12, 14.49, 14.45, 11.79. FTIR (KBr) ν 929, 1215, 1508, 1539, 1558, 1575, 2148, 2399 cm^{-1}. EM m/z 1861, 1838, 1755, 1672, 1492, 1317, 1201. λ_{max} (CH_2Cl_2): 433; 272 nm. Anal. Calcd for $C_{120}H_{182}O_{10}Si_2$: C 78.29, H 9.96. Found: C 77.52, H 9.76%.

Compound 9

Compound **8** (155 mg, 0.085 mmol) was dissolved in THF (15 mL) and tetrabutylammonium fluoride (0.17 mL, 0.179 mmol) was added to the solution. The solution was stirred at room temperature for 12 h. The mixture was extracted with chloroform and washed with water. The organic phase was dried with $MgSO_4$. The solvent was removed and the product was crystallization with hexane. Yield 98% of yellow solid. Mp 95–96 °C. ^{1}H NMR (300 MHz, $CDCl_3$) δ: 7.02–7.00 (brs, 10H), 4.05–4.00 (m, 20H), 3.36 (s, 2H), 1.85–1.81 (m, 20H), 1.58–1.52 (m, 20H), 1.40–1.26 (m, 40H), 0.92–0.89 (m, 30H). ^{13}C NMR (75 MHz, $CDCl_3$) δ: 155.36, 154.53, 153.89, 153.69, 118.30, 118.17, 117.60, 117.41, 115.80, 115.34, 114.78, 114.67, 114.52, 112.92, 92.00, 91.96, 91.62, 82.71, 80.45, 79.75, 76.99, 70.29, 70.11, 70.05, 32.02, 31.94, 30.11, 29.69, 29.64, 29.54, 26.08, 26.05, 26.02, 23.05, 14.45. FTIR (KBr) ν 1265, 2304, 2385, 3419 cm^{-1}. EM m/z 1549, 1443, 1361, 1201, 1088.

Compound 10c

Compound **9** (63 mg, 0.041 mmol) and **5** (19.03 mg, 0.082 mmol) were dissolved in dry THF (20 mL), and the system was flushed with argon. Tetrakis(triphenylphosphine)-palladium (4.76 mg, 0.004 mmol), copper(I) iodine (0.5 mg, 0.004 mmol) were added. The mixture was heated for 46 h at 70–80 °C. Chloroform was added to the residue and washed with saturated NH_4Cl, HCl (10%) and NaCl. The organic phase was dried with $MgSO_4$ and the solvent was removed. The crude product was purified by column chromatography on silica gel (hexane–AcOEt 9 : 1). Yield 43% of yellow-orange solid. Mp 119–120 °C. ^{1}H NMR (200 MHz, $CDCl_3$) δ: 10–03 (s, 2H), 7.89–7.87 (d, J = 8.09 Hz, 4H), 7.70–7.67 (d, J = 8.09 Hz, 4H), 7.03 (s, 10H), 4.08–4.02 (t, J = 6.45 Hz, 20H), 2.05–1.82 (m, 20H), 1.81–1.56 (m, 20H), 1.54–1.23 (m, 40H), 0.9–0.84 (m, 30H). ^{13}C NMR (50 MHz, $CDCl_3$) δ: 191.45, 153.91, 153.54, 153.50, 153.45, 135.32, 132.01, 129.85, 129.59, 117.23, 117.08, 116.94, 115.26, 114.47, 114.29, 114.09, 112.92, 93.92, 92.05, 91.68, 91.68, 91.56, 91.34, 90.33. FTIR (KBr) ν 731, 777, 1024, 1217, 1274, 1386, 1493, 1596, 1654, 1701, 2854, 2925. λ_{max} (CH_2Cl_2): 432.99, 324.01, 279 nm. EM m/z 1735.

Triad 11c

To a solution of C_{60} (76.32 mg, 0.106 mmol) was dissolved in chlorobenzene (50 mL), compound **10c** (93 mg, 0.053 mmol) and sarcosine (14.15 mg, 0.159 mmol) was added. The mixture was heated under reflux for 3 h. After the evaporation the solvent, the residue was purified by column chromatography on silica gel (CS_2–toluene 5 : 2). Yield 13% of black solid. ^{1}H NMR (500 MHz, $CDCl_3$) δ: 7.74 (brs, 2H), 7.73–7.72 (d, J = 3.33 Hz, 2H), 7.63–7.56 (d, J = 8.15 Hz, 4H), 7.03–7.01 (s, 10H), 4.06–4.02 (m, 20H), 2.85 (s, 3H), 1.70–1.60 (m, 20H), 1.58–1.45 (m, 20H), 1.4–1.2 (m, 40H), 0.92–0.75 (m, 30H). ^{13}C NMR (125 MHz, $CDCl_3$) δ: 168.15, 156.56, 154.34, 154.06, 153.93, 153.90, 153.61, 153.44, 147.73, 147.06, 146.84, 146.74, 146.69, 146.64, 146.57, 146.52, 146.44, 146.37, 146.35, 146.17, 145.95, 145.84, 145.75, 145.69, 145.65, 145.59, 145.11, 145.03, 144.79, 143.56, 143.50, 143.41, 143.11, 143.01, 142.99, 142.96, 142.68, 142.65, 142.53, 142.45, 142.31, 142.10, 141.96, 140.57, 140.30, 140.00, 137.71, 137.26, 136.89, 136.30, 136.12, 132.87, 131.26, 129.20, 117.70, 117.50, 114.88, 114.75, 114.70, 114.19, 91.99, 91.89, 83.75, 70.46, 70.11, 70.01, 69.48, 68.56, 40.41, 39.14, 32.33, 32.02, 32.01, 31.99, 31.31, 30.77, 30.10, 30.06, 29.76, 29.71, 29.33, 26.13, 26.08, 26.06, 24.16, 23.38, 23.09,

23.03, 14.51, 14.47, 14.44, 14.43, 11.36. λ_{max} (CH_2Cl_2): 430.9, 311.98, 255.94 nm. EM *m*/*z* 1616, 1524, 1373, 969.

Acknowledgements

The authors acknowledge the Secretaría de Estado de Educación y Universidades and MECD of Spain. This work has been supported by the MCYT of Spain (Projects BQU2002-00855, BQU2000-0790). Part of this work was carried out with support from the EU (RTN network "WONDERFULL") SFB 583 and the Office of Basic Energy Sciences of the U.S. Department of Energy (Contribution No. NDRL-4580 from the Notre Dame Radiation Laboratory).

Carmen Atienza,[a] Braulio Insuasty,[ab] Carlos Seoane,[a] Nazario Martín,*[a] Jeff Ramey,[c] G. M. Aminur Rahman[d] and Dirk M. Guldi*[c]
[a]*Departamento de Química Orgánica, Facultad de Ciencias Químicas, Universidad Complutense, E 28040 Madrid, Spain. E-mail: nazmar@quim.ucm.es; Fax: 91 394 4103; Tel: 91 394 4227*
[b]*Departamento de Química, Facultad de Ciencias, Universidad del Valle, AA-25360, Cali, Colombia*
[c]*Universität Erlangen, Institute for Physical Chemistry, 91058 Erlangen, Germany. E-mail: dirk.guldi.@chemie.uni-erlangen.de*
[d]*Radiation Laboratory, University of Notre Dame, Notre Dame, IN 46556, USA*

References

1 (*a*) *An Introduction to Molecular Electronics*, ed. M. C. Petty, M. R. Bryce and D. Bloor, Oxford University Press, New York, 1995; (*b*) P. F. Barbara, T. J. Meyer and M. A. Ratner, *J. Phys. Chem.*, 1996, **100**, 13148; (*c*) *Molecular Electronics*, ed. J. Jortner and M. Ratner, Blackwell, Oxford, 1997.
2 V. Balzani, M. Veaturi and A. Credi, *Molecular Devices and Machines. A Journey into the Nanoworld*. Wiley-VCH, Weinheim, Germany, 2003.
3 (*a*) N. C. Greenham, S. C. Moratti, D. D. C. Bradley, R. H. Friend and A. B. Holmes, *Nature*, 1993, **365**, 628; (*b*) W. R. Salaneck, I. Lundström and B. Ranby, *Conjugated Polymers and Related Materials*, Oxford University Press, Oxford, 1993; (*c*) K. Müllen, *Pure Appl. Chem.*, 1993, **65**, 89; H. E. Katz, S. F. Bent, W. L. Wilson, M. L. Schilling and S. B. Ungashe, *J. Am. Chem. Soc.*, 1994, **116**, 6631; (*d*) J. M. Tour, *Chem. Rev.*, 1996, **96**, 537; (*e*) A. Kraft, A. C. Grimsdale and A. B. Holmes, *Angew. Chem., Int. Ed.*, 1998, **37**, 403; (*f*) U. Scherf, *Top. Curr. Chem.*, 1999, **201**, 163–222; (*g*) R. E. Martin and F. Diederich, *Angew. Chem., Int. Ed.*, 1999, **38**, 1350; (*h*) J. L. Segura and N. Martín, *J. Mater. Chem.*, 2000, **10**, 2403.
4 K. Müllen and G. Wegner, *Electronic Materials: The Oligomer Approach*, Wiley-VCH, Weinheim Germany, 1998.
5 L. Echegoyen and L. E. Echegoyen, *Acc. Chem. Res.*, 1998, **31**, 593–601.
6 (*a*) N. Martín, L. Sánchez, B. Illescas and I. Pérez, *Chem. Rev.*, 1998, **98**, 2527; (*b*) H. Imahori and Y. Sakata, *Eur. J. Org. Chem.*, 1999, **10**, 2445–2457; (*c*) *From Synthesis to Optoelectronic Properties*, ed. D. M. Guldi and N. Martín, Kluwer Academic Publishers, Dordrecht, The Netherlands, 2002; (*d*) D. M. Guldi, *Chem. Commun.*, 2000, 321–327; (*e*) D. M. Guldi and N. Martín, *J. Mater. Chem.*, 2002, **12**, 1978–1992; (*f*) D. M. Guldi and M. Prato, *Chem. Commun.*, 2004, 2517–2525.
7 (*a*) J. L. Segura, N. Martín and D. M. Guldi, *Chem. Soc. Rev.*, 2005, in press; (*b*) J. F. Nierengarten, *Solar Energy Mater. Solar Cells.*, 2004, **83**, 187–199.
8 (*a*) P. A. van Hal, J. Knol, B. M. W. Langeveld-Voss, S. C. J. Meskers, J. C. Hummelen and R. A. J. Janssen, *J. Phys. Chem. A*, 2000, **104**, 5974–5988; (*b*) E. H. A. Beckers, P. A. van Hal, A. Dhanabalan, S. C. J. Meskers, J. Knol, J. C. Hummelen and R. A. J. Janssen, *J. Phys. Chem. A*, 2003, **107**, 6218–6224; (*c*) A. M. Ramos, S. C. J. Meskers, P. A. van Hal, J. Knol, J. C. Hummelen and R. A. J. Janssen, *J. Phys. Chem. A*, 2003, **107**, 9269–9283.
9 (*a*) D. M. Guldi, C. Luo, A. Swartz, R. Gomez, J. L. Segura, N. Martin, C. Brabec and N. Sariciftci, *J. Org. Chem.*, 2002, **67**, 1141–1152; (*b*) F. Giacalone, J. L. Segura and N. Martín, *J. Org. Chem.*, 2002, **67**, 3529–3532; (*c*) D. M. Guldi, C. Luo, A. Swartz, R. Gomez, J. L. Segura and N. Martin, *J. Phys. Chem. A*, 2004, **108**, 455–467.
10 F. Giacalone, J. L. Segura, N. Martín and D. M. Guldi, *J. Am. Chem. Soc.*, 2004, **126**, 5340–5341.
11 K. Komatsu, Y. Murata, N. Takimoto, S. Mori, N. Sugita and S. M. Wan, *J. Org. Chem.*, 1994, **59**, 6101.
12 (*a*) J.-F. Eckert, J.-F. Nicoud, J.-F. Nierengarten, S.-G. Liu, L. Echegoyen, N. Armaroli, F. Barigelletti, L. Ouali, V. Krasnikov and G. Hadziioannou, *J. Am. Chem. Soc.*, 2000, **122**, 7467–7479; (*b*) S. Fukuzumi, H. Imahori, H. Yamada, M. E. El-Khouly, M. Fujitsuka, O. Ito and D. M. Guldi, *J. Am. Chem. Soc.*, 2001, **123**, 2571–2575.
13 Y. Shirai, Y. Zhao, L. Cheng and J. M. Tour, *Org. Lett.*, 2004, **6**, 2129–2132.
14 (*a*) M. Maggini, G. Scorrano and M. Prato, *J. Am. Chem. Soc.*, 1993, **115**, 9798–9799; (*b*) M. Prato and M. Maggini, *Acc. Chem. Res.*, 1998, **31**, 519–526; (*c*) N. Tagmatarchis and M. Prato, *Synlett*, 2003, 6.
15 (*a*) D. Ickenroth, S. Weissmann, N. Rumpf and H. Meier, *Eur. J. Org. Chem.*, 2002, **16**, 2808–2814; (*b*) H. Meier, D. Ickenroth, U. Stalmach, K. Koynov, A. Bahtiar and C. Bubeck, *Eur. J. Org. Chem.*, 2001, **23**, 4431–4443.
16 Q. Zhou, P. J. Carroll and T. M. Swager, *J. Org. Chem.*, 1994, **59**, 1294.
17 H. Meier, D. Ickenroth, U. Stalmach, K. Koynov, A. Bahtiar and Ch. Bubeck, *Eur. J. Org. Chem.*, 2001, 4431–4443.
18 M. Segura, L. Sánchez, J. de Mendoza, N. Martín and D. M. Guldi, *J. Am. Chem. Soc.*, 2003, **125**, 15093–15100.
19 C. Martineau, P. Blanchard, D. Rondeau, J. Delaunay and J. Roncali, *Adv. Mater.*, 2002, **14**, 283.
20 T. Suzuki, Y. Maruyama, T. Akasaba, W. Ando, K. Kobayashi and S. Nagase, *J. Am. Chem. Soc.*, 1994, **116**, 1359–1363.
21 D. M. Guldi and M. Prato, *Acc. Chem. Res.*, 2000, **33**, 695.
22 No notable phosphorescence is seen in the 600–800 nm region.
23 D. M. Guldi, *Chem. Soc. Rev.*, 2002, **31**, 22–36.
24 F. Hauke, A. Hirsch, S. G. Liu, L. Echegoyen, A. C. Swartz Luo and D. M. Guldi, *ChemPhys Chem*, 2003, **3**, 195.

